frontiers in Environmental Science

ORIGINAL RESEARCH
published: 13 April 2021
doi: 10.3389/fenvs.2021.650539

# Changes in Urban Gas-Phase Persistent Organic Pollutants During the COVID-19 Lockdown in Barcelona

*Raimon M. Prats*, Barend L. van Drooge, Pilar Fernández, Esther Marco and Joan O. Grimalt*

*Institute of Environmental Assessment and Water Research (IDAEA-CSIC), Barcelona, Spain*

The composition of polycyclic aromatic hydrocarbons (PAHs), polychlorobiphenyls (PCBs), hexachlorobenzene (HCB), pentachlorobenzene (PeCB), and organophosphate flame retardants (OPFRs) present in the gas-phase fraction of the atmosphere of Barcelona was analyzed during the SARS-CoV-2 coronavirus disease (COVID-19) lockdown and prior to this period. The changes in daily concentrations of CO, NO, $NO_2$, $O_3$ and particulate matter smaller than 10 μm ($PM_{10}$) were considered for comparison. Bayesian analysis considering serial dependencies and seasonality showed statistically significant decreases of CO, NO, $NO_2$, and $PM_{10}$ (between −28 and −76%) and $O_3$ increases (+45%) during lockdown. However, the lockdown concentration decreases of PeCB (−90.5%, from 8.5 to 0.8 pg $m^{-3}$), HCB (−79%, 25.5–5.4 pg $m^{-3}$) and some PAHs, such as benz[a]anthracene (−87%, 120–17 pg $m^{-3}$) and pyrene (−81%, 3,500–680 pg $m^{-3}$), were even stronger. The PAH depletion ranged between −68 and −87% that could be primarily associated with the strong reduction of traffic mobility during this period (−80%). Besides traffic reduction, the observed air quality improvements could be related to lower generation of solid urban residues (−25%) and the subsequent decrease of urban waste incineration (between −25 and −28%). Tributyl phosphate also showed a reduction in concentration during lockdown but the other OPFRs were seemingly not affected by this restriction, possibly as a result of the uniform release from the emission sources, e.g., construction material, industrial applications, and household products.

**Keywords: COVID-19, semi-volatile air pollutants, organic contaminants, passive air sampling, lockdown, air quality**

OPEN ACCESS

***Edited by:***
*Dimitris G. Kaskaoutis, National Observatory of Athens, Greece*

***Reviewed by:***
*Umesh Dumka, Aryabhatta Research Institute of Observational Sciences, India*
*Suvarna Sanjeev Fadnavis, Indian Institute of Tropical Meteorology, India*

****Correspondence:***
*Raimon M. Prats*
*raimon.martinez@idaea.csic.es*

***Specialty section:***
*This article was submitted to Atmosphere and Climate, a section of the journal Frontiers in Environmental Science*

***Received:*** *07 January 2021*
***Accepted:*** *23 March 2021*
***Published:*** *13 April 2021*

***Citation:***
*Prats RM, van Drooge BL, Fernández P, Marco E and Grimalt JO (2021) Changes in Urban Gas-Phase Persistent Organic Pollutants During the COVID-19 Lockdown in Barcelona. Front. Environ. Sci. 9:650539. doi: 10.3389/fenvs.2021.650539*

## INTRODUCTION

The outbreak of a novel respiratory disease in China, caused by the SARS-CoV-2 virus and named coronavirus disease (COVID-19) by the World Health Organization (WHO), was quickly extended to many other countries generating a global pandemic (Sohrabi et al., 2020). On March 14, a lockdown was set in all Spain which mandated individuals to remain home except for needs such as purchasing food and medicines. These measures also included the temporary closure of schools, universities, some businesses and shops.

In general, lockdown measures have led to unprecedented reductions of air pollutant concentrations in many regions of the world, including several of the most polluted areas

(Berman and Ebisu, 2020; Cameletti, 2020; Le Quéré et al., 2020; Li et al., 2020; Venter et al., 2020; Zhang R. et al., 2020; Zhang Z. et al., 2020). Most reports in urban and industrial areas have only focused on air quality gas pollutants such as nitrogen oxides (NO and $NO_2$), carbon monoxide (CO), and carbon dioxide ($CO_2$), and particulate matter ($PM_{10}$ and $PM_{2.5}$). The same is the case for satellite imaging methods that can estimate the concentrations of these gases over large geographical areas (Kaufman et al., 1997; Krotkov et al., 2016). However, pollution assessment also requires the measurement of other contaminants that are deleterious for human health, such as organochlorine compounds (OCs) and polycyclic aromatic hydrocarbons (PAHs), among others.

Most OCs and PAHs are persistent organic pollutants (POPs), a group of compounds that are notorious for their resistance to degradation, potential for long-range atmospheric transport, and toxicity. They are recognized as a threat to human and wildlife health (De Voogt et al., 1990; Grimalt et al., 1994; Boström et al., 2002; Lauby-Secretan et al., 2013). PAHs are of great environmental concern, since several parent (non-methylated) compounds of these hydrocarbons are human carcinogens and priority pollutants (Baek et al., 1991; Armstrong et al., 2004). Hexachlorobenzene (HCB) has been related with obesity (Smink et al., 2008; Valvi et al., 2014), low fetal growth (Lopez-Espinosa et al., 2016), disruption of thyroid metabolism (Sala et al., 2001; Llop et al., 2017), and higher incidence of thyroid cancer (Grimalt et al., 1994). Polychlorobiphenyls (PCBs) have also been related with low fetal growth (Casas et al., 2015; Lopez-Espinosa et al., 2016), obesity (Valvi et al., 2012) or alterations of the thyroid function (Chevrier et al., 2008). In addition, they have been associated with metabolic disturbances of 25-hydroxy-vitamin D3 (Morales et al., 2013) and neurotoxicity (Grandjean and Landrigan, 2014). The production and use of these compounds have been restricted in many industrialized countries, resulting in significant endeavors to gradually reduce and prevent their release and diffusion in the environment. A culminating protocol for the elimination and monitoring of POPs was elaborated in 2001 during the Stockholm Convention[1] and has since been amended to include more compounds.

In addition, organophosphate flame retardants (OPFRs) are emerging pollutants that are currently used and produced in increasing amounts to meet the demand for flame retardants and plasticizers in construction material, industrial applications, and household products, including electronic devices (Van der Veen and de Boer, 2012; Du et al., 2019). OPFRs are neurotoxic, may cause haemolysis, and some of them are carcinogenic (Dishaw et al., 2011; Van der Veen and de Boer, 2012). Compared to historical POPs, OPFRs tend to show relatively high concentrations in outdoor air from urban and industrial areas (Salamova et al., 2014; Liu et al., 2016; van Drooge et al., 2018b).

Barcelona is one of the most densely populated cities of Europe, 16,000 inhabitants/$km^2$. Its metropolitan area lacks significant atmospheric emissions from industries and domestic heating is generally powered by natural gas. The high traffic intensity, 13,000–85,000 vehicles/day downtown in 2018, is the main pollution source (van Drooge and Grimalt, 2015; van Drooge et al., 2018a). Other reports (UNEP, 2010) also point at transport, housing, and related activities as important sources of emissions of pollutants and products of environmental concern in Spain (e.g., around 60% of $CO_2$ and greenhouse gasses are emitted from transport and housing-related activities). Air pollution is therefore closely related to the activities of its inhabitants. Comparison of the air pollution levels during regular days and the lockdown period may provide guidelines for the ultimate achievable air quality standards, namely POPs, upon ideal management of urban pollution sources. Air samples were collected in the atmosphere of the city of Barcelona by means of passive air sampling (PAS) during regular conditions and lockdown. The results were used to determine possible changes in gas-phase POP concentrations during both periods. These pollutants were also analyzed in a remote continental background location in the Pyrenees for PAS calibration and comparison with the lockdown atmospheric conditions.

# MATERIALS AND METHODS

## Air Sampling

Two passive gas-phase air samplers for POP analysis were deployed during two periods: B1 (15 October 2019–9 January 2020, 86 days) and B2 (9 January 2020–15 July 2020, 188 days). B1 provided a reference time interval of typical air pollution conditions in the city. B2 was deployed during lockdown, although this period was larger than the specific lockdown time (March 15–June 22, 2020, 100 days). The samples were obtained using GAPS-style polyurethane foam passive air samplers (PUF-PASs) as employed in other studies (e.g., Pozo et al., 2009). The PUF disks (14 cm diameter, 1.35 cm thickness, 369.5 $cm^2$ surface area, and 0.021 g $cm^{-3}$ density) were previously cleaned with acetone, Soxhlet-extracted with hexane for 6 h, dried under vacuum, and stored in a sealed PET/LLDPE bag at −20°C. Upon deployment, they were spiked with a Performance Reference Compound (PRC) mixture of PCBs 3, 9, 15, 32 (all $^{13}$C-labeled), 107, and 198 (unlabeled) (Cambridge Isotope Laboratories, Tewksbury, United States). One field blank was performed for each sample. These blanks were also doped with the PRCs, sealed, and stored at −20°C for the entire duration of the sampling period. The PUFs were immediately extracted after retrieval at the end of the sampling period. The recovery of PRCs from each sample was used for the assessment of the specific sampling rates as explained in the "Theory and Calculations" section below.

Polyurethane foam passive air samplers were also deployed in duplicate, in four 4–10-month periods, at six remote locations in the Pyrenees (September 2017–September 2019). Because of the minimal local contaminant sources, these sites constitute continental background reference regions for air pollution levels. The results obtained with the PUF-PASs were evaluated by comparison with those from active air sampling (AAS) with a high-volume pump (MCV, Collbató; van Drooge et al., 2004) which was used in one of these Pyrenean sites between July and September 2017. The PUF-AAS plugs (6 cm diameter, 5 cm thickness, 0.028 g $cm^{-3}$ density) used for this purpose were

[1] www.pops.int

located behind glass fiber filters that collected the atmospheric particle phase. One field blank was performed for every two duplicate samplers, both for PAS and AAS. All PUFs were cleaned and stored until extraction as described above.

Meteorological and air quality data were obtained for the whole B1 and B2 periods, including the pre- and lockdown intervals within them. Data corresponding to analogous periods in the previous 2 years were also collected for reference and description of seasonal variations. **Table 1** summarizes temperature, accumulated precipitation, and wind speed average values recorded on-site in all locations with Tinytag Plus 2 data loggers (Gemini Data Loggers, Chichester, United Kingdom) and from the automatic meteorological network (XEMA stations VS, Z2, X8, and X4) of the Catalan Meteorological Service. The concentrations of CO, NO, $NO_2$, $PM_{10}$, and $O_3$ in Barcelona were obtained for the same periods from the stations of the Air Quality Network (XVPCA 08019043 and 08019057) of the Catalan Government.

## Extraction and Clean-Up

Both the PUF-PAS disks and the PUF-AAS plugs were subjected to Soxhlet extraction with hexane (Merck, Darmstadt, Germany) for 6 h after being spiked with a mixture of recovery standards containing: tetrabromobenzene, PCB209, fluorene-$d_{10}$, phenanthrene-$d_{10}$, fluoranthene-$d_{10}$, pyrene-$d_{10}$, benz[a]anthracene-$d_{12}$, and chrysene-$d_{12}$ (Dr. Ehrenstorfer) as well as an alkyl/aryl phosphate mixture containing tributyl phosphate-$d_{12}$, tris(2-chloroethyl) phosphate-$d_{12}$, tris(1-chloro-2-propyl) phosphate-$d_{18}$, tris(1,3-dichloro-2-propyl) phosphate-$d_{15}$ and triphenyl phosphate-$d_{15}$ (Cambridge Isotope Laboratories). The extracts were concentrated down to 2 mL with a rotary evaporator (Büchi, Flawil, Switzerland), quantitatively transferred into gas chromatography vials, and further evaporated to 0.5 mL under a gentle stream of nitrogen.

Fifty μL of each extract were cleaned-up and fractionated using an Agilent 1200 Series Gradient HPLC system (Agilent Technologies, Santa Clara, United States) equipped with a quaternary pump, a vacuum degasser, an autosampler, a thermostated column compartment (set at 30°C), and a preparative fraction collector. A Tracer Excel 120 SI HPLC silica column (25 cm × 3 μm × 0.46 cm i.d.; Teknokroma, Sant Cugat del Vallès) was used for the chromatographic separation. The elution program was as follows: 100% hexane at 0.5 mL $min^{-1}$ flow rate for 8 min, then a linear gradient to 100% dichloromethane at 0.5 mL $min^{-1}$ in 7 min, held until min 20. It was additionally changed to (80:20%) dichloromethane:methanol in order to elute more polar compounds remaining in the column before performing the next fractionation, with a linear flow rate increase from 0.5 to 1 mL $min^{-1}$ in 10 min, and a final holding time of 15 min. The fractions containing the target compounds were collected between minutes 8–15 (PCBs and other OCs) and 15–20 (PAHs). These fractions were evaporated under a gentle nitrogen gas stream, transferred into gas chromatography vials, and further evaporated to 0.5 mL. The OPFRs were analyzed from another extract aliquot, not requiring HPLC fractionation, but dried by elution through 0.5 g of anhydrous sodium sulfate previously activated overnight at 450°C.

## Instrumental Analysis

The OC and PAH HPLC fractions were run separately by gas chromatography coupled to mass spectrometry (GC-MS) with a Thermo Trace GC Ultra–DSQ II (Thermo Fisher Scientific, Waltham, United States) equipped with a 60 m × 0.25 mm i.d. × 25 μm film thickness HP-5MS fused capillary column (Agilent Technologies). The MS was operated in electron impact mode (70 eV). The injector, ion source, quadrupole, and transfer line temperatures were 280, 250, 150, and 270°C, respectively. The oven program started at 90°C with a hold time of 1 min, then heated to 150°C at 10°C $min^{-1}$ and to 320°C at 6°C $min^{-1}$, where it was held for 20 min. Helium was used as a carrier gas at 1 mL $min^{-1}$. The targeted compounds were the following: polychlorobiphenyls (PCB28, PCB52, PCB101, PCB118, PCB138, PCB153, and PCB180), HCB, pentachlorobenzene (PeCB), $\alpha$- and $\gamma$-hexachlorocyclohexanes ($\alpha$- and $\gamma$-HCH), fluorene (fle), phenanthrene (phe), fluoranthene (flu), pyrene (pyr), benz[a]anthracene (b[a]ant), and chrysene+triphenylene (chr+triph). They were identified by their m/z values and retention times recorded in selected ion monitoring (SIM) mode (**Supplementary Table 1**).

The PUF extract aliquots were run for OPFR analysis by gas chromatography coupled to tandem mass spectrometry (GC-MS/MS) into an Agilent 7000 Series Triple Quad GC/MS (Agilent Technologies) equipped with a 30 m × 0.25 mm i.d. × 0.25 μm film thickness Zebron ZB-PAH capillary column (Phenomenex, Torrance, CA, United States). The MS/MS was operated in electron impact ionization mode. The injector, ion source, quadrupoles, and transfer line temperatures were 280, 230, 150, and 280°C, respectively. The oven temperature program started at 80°C with a hold time of 1.5 min, then heated to 220°C at 10°C $min^{-1}$ and to 315°C at 15°C $min^{-1}$, where it was held for 5 min. Helium was used as a carrier gas at 1.1 mL $min^{-1}$. The targeted compounds were the following: tributylphosphate (TBP), tris(2-chloroethyl) phosphate (TCEP), tris(1-chloro-2-propyl) phosphate (TCPP), tris(1,3-dichloro-2-propyl) phosphate (TDCP) and triphenyl phosphate (TPhP). They were identified by their m/z transitions and retention times recorded in multiple reaction monitoring mode (**Supplementary Table 2**).

Quantification was performed with internal standard calibration curves, accounting for extraction and analysis recoveries. The field blank values were subtracted. LOQ values ranged between 0.5 and 2.5 pg in column, or 125–625 pg/sampler for PAHs, OCs, and PCBs, and 250–1,250 pg/sampler for OPFRs. For average effective sampled air volumes, these correspond to 0.3–1.6 pg $m^{-3}$ of air for PAHs, 0.4–2.1 pg $m^{-3}$ for OCs, 0.2–1.2 pg $m^{-3}$ for PCBs, and 0.5–2.4 pg $m^{-3}$ for OPFRs.

## Theory and Calculations

As shown in Equation 1 (Harner et al., 2013), the calculation of gas-phase concentrations ($C_A$, pg $m^{-3}$) from the pollutant amounts obtained with PAS ($N_A$) requires the determination of effective sampled volumes ($V_A$, $m^3$) that are compound- and location-specific for each sampling period:

**TABLE 1 |** Sampling locations, periods of study, and average meteorological conditions (± standard deviation).

| Location | | Altitude (m.a.s.l.) | Period | | Temperature (°C) | Precipitation (mm) | Wind speed (m $s^{-1}$) |
|---|---|---|---|---|---|---|---|
| Barcelona (urban site) | 41.388° N, 2.115° E | 108 | Mean 2018–2019 | B1 | 14.3 ± 0.2 | 197 ±114 | 1.21 ±0.21 |
| | | | | B2 | 16.5 ± 0.1 | 257 ± 155 | 1.23 ± 0.02 |
| | | | | Pre-lockdown | 11.8 ± 0.2 | 90 ± 91 | 1.30 ± 0.19 |
| | | | | Lockdown | 17.4 ± 0.6 | 166 ± 73 | 1.25 ± 0.03 |
| | | | 2020 | B1 | 14.7 ± 3.6 | 225 | 1.99 ± 1.46 |
| | | | | B2 | 17.3 ± 5.0 | 513 | 2.15 ± 1.39 |
| | | | | Pre-lockdown | 13.1 ± 2.6 | 124 | 2.12 ± 1.62 |
| | | | | Lockdown | 18.0 ± 4.0 | 373 | 2.15 ± 1.26 |
| Aigüestortes (continental background) | 42.572° N, 0.932° E | 1,619–2,453 | 2017–2019 | Range of averages[a] | 4.7 ± 0.2–8.3 ± 0.7 | 484 ± 330–1,832 ± 389 | 3.70 ± 1.00–4.27 ± 0.05 |

[a]*Values for temperature, accumulated precipitation, and wind speed for the sampling site of Aigüestortes are shown as a range spanning the lowest and highest average values (± standard deviation) registered over four consecutive 4–10-month sampling periods from six studied mountain locations.*

$$C_A = \frac{N_A}{V_A} = \frac{N_A}{V_{PUF}\, K'_{PUF-A}\left[1 - exp\left(\frac{-k_A\, t}{K'_{PUF-A}\, D_{film}}\right)\right]} \quad (1)$$

where $N_A$ is the amount of compound accumulated in the PUF disk during the sampling time (pg sampler$^{-1}$), $V_{PUF}$ is the volume of the PUF disk (0.00021 m$^3$), $K'_{PUF-A}$ is the dimensionless PUF density-corrected PUF-Air partition coefficient $K_{PUF-A}$ ($K_{PUF-A}$ multiplied by the PUF density, $\delta_{PUF}$ = 21,000 g m$^{-3}$), $k_A$ is the air-side mass transfer coefficient (m d$^{-1}$), t is the sampling time (d), and $D_{film}$ is the PUF's effective film thickness (0.00567 m).

The sample-specific $k_A$ values needed for $V_A$ estimation can be derived from the PRC calibration of sampling rates ($R_S$, m$^3$ d$^{-1}$):

$$k_A = \frac{R_S}{A_{PUF}} = \frac{\ln(C/C_0)\; K'_{PUF-A}\, D_{film}}{t} \quad (2)$$

where $A_{PUF}$ is the PUF's surface area (0.0365 m$^2$) and $C/C_0$ is the PCR ratio of amounts (g sampler$^{-1}$) between exposed and non-exposed (field blanks) PUFs.

Compound-specific $K_{PUF-A}$ values for this type of PUFs are correlated to octanol-air partition coefficients ($K_{OA}$) through the following relationship (Shoeib and Harner, 2002):

$$\log K_{PUF-A} = 0.6366 \log K_{OA} - 3.1774 \quad (3)$$

The $\log K_{OA}$ values were corrected for the average temperature of each sampling site over the sampling period using temperature-dependent relationships reported elsewhere (Odabasi et al., 2006; Chen et al., 2016; Harner, 2016; Wang et al., 2017).

# RESULTS AND DISCUSSION

## Passive Gas-Phase Air Sampling for POP Analysis

The performance of the PUF-PAS samplers and reliability of the pollutant concentrations obtained with this system were assessed by comparison of the results from simultaneous deployment of these PAS and AAS between September 2017 and September 2019 in Aigüestortes, a continental background location in remote high mountains. The quantitative results obtained with both methods were in good agreement (**Table 2**). Thus, the AAS/PAS ratio differences were 0.7–2.1 for PCBs, 1.1 for HCB, 0.3–0.8 for PAHs and 0.3–1.5 for OPFRs. These ratios have to be compared considering that AAS involves much more variability than PAS, as the former is only collected over a few hours and the latter represents average values of several months of deployment. Therefore, variations in day-to-day meteorological and atmospheric conditions greatly affect the resulting AAS levels, especially for compounds like PAHs that could be influenced by local sources from nearby rural areas that are much more season dependent. Thus, the differences between sampling methods were deemed to be within acceptable ranges, especially at the low observed concentrations, for all compounds < 50 pg m$^{-3}$ except for Fle and Phe. These results concur with other studies that established a strong agreement or no statistical difference between AAS- and PAS-obtained concentrations, even in urban sites with generally higher POP concentrations (He and Balasubramanian, 2012; Kalina et al., 2019). Furthermore, PAS duplicates showed low average relative standard deviations (RSD), between 9.4 and 23.3% for most compounds, with values above 30% only observed for the less volatile compounds such as PCB180, TCPP, TCEP, and TDCP, 34.2, 30.8, 36.3, and 60.1%, respectively (**Supplementary Table 3**).

## Urban Concentrations of Organochlorine Compounds, PAHs, and Organophosphate Flame Retardants

The concentrations of HCB found in the B1 and B2 periods in Barcelona, 25.5 and 5.4 pg m$^{-3}$, respectively (**Table 2**), were generally lower than those found in other urban areas from India: average values of 120–260 pg m$^{-3}$ (Chakraborty et al., 2010), Bangladesh: 70–685 pg m$^{-3}$ (Nost et al., 2015), Bosnia Herzegovina: 34 pg m$^{-3}$ (Lammel et al., 2011), Nepal: 6.3–1,500 pg m$^{-3}$ (Pokhrel et al., 2018), or China: 261 pg m$^{-3}$ (Zhang et al., 2010). The concentrations of PeCB, 8.5 and 0.8 pg m$^{-3}$ in B1 and B2, respectively, were

**TABLE 2 |** Average compound concentrations in air (gas phase, pg $m^{-3}$ ± standard deviation) in the mountain background (Aigüestortes) and in the urban (Barcelona) locations, obtained using passive air sampling (PAS), and active air sampling (AAS) methods.

| Compounds | | Aigüestortes (background) | | | | Barcelona PAS (urban) | | |
|---|---|---|---|---|---|---|---|---|
| | | PAS (*n* = 20) | | AAS (*n* = 3) | | B1 | B2 | Variation % |
| PCBs | PCB28 | 2.9 | ±1.0 | 2.4 | ±1.5 | 6.8 | 2.8 | −59 |
| | PCB52 | 2.1 | ±0.7 | 1.4 | ±0.3 | 11 | 3.4 | −68 |
| | PCB101 | 2.7 | ±1.0 | 5.7 | ±1.9 | 15 | 6.1 | −59 |
| | PCB118 | 2.5 | ±0.3 | 4.8 | ±1.6 | 13 | 3.9 | −69.5 |
| | PCB138 | 1.6 | ±0.7 | 3.0 | ±0.9 | 6.7 | 4.4 | −34 |
| | PCB153 | 2.3 | ±0.2 | 3.2 | ±0.9 | 5.8 | 2.6 | −56 |
| | PCB180 | 0.5 | ±0.2 | 0.5 | ±0.1 | b.d.l.[a] | b.d.l. | |
| | ΣPCBs | 14.6 | | 21.0 | | 58.3 | 23.2 | −60 |
| OCs | HCB | 45 | ±8.4 | 49 | ±4.9 | 25.5 | 5.4 | −79 |
| | PeCB | 25 | ±3.2 | b.d.l. | | 8.5 | 0.8 | −90.5 |
| | α-HCH | 1.6 | ±0.3 | b.d.l. | | 3.5 | 0.5 | −86 |
| | γ-HCH | 1.0 | ±0.4 | b.d.l. | | 12.9 | 3.9 | −70 |
| | ΣOCs | 72.6 | | 49.0 | | 50.4 | 10.6 | −79 |
| PAHs | Fle | 250 | ±38 | 72 | ±3.6 | 10,000 | 2,600 | −75 |
| | Phe | 300 | ±88 | 230 | ±170 | 18,000 | 5,800 | −68 |
| | Flu | 39 | ±16 | 28 | ±14 | 4,000 | 1,000 | −75 |
| | Pyr | 18 | ±7.6 | 15 | ±6.7 | 3,500 | 680 | −81 |
| | B[a]ant | 0.7 | ±0.5 | 0.3 | ±0.1 | 120 | 17 | −87 |
| | Chr+TriPh | 5.3 | ±2.8 | 1.4 | ±0.1 | 240 | 63.5 | −74 |
| | ΣPAHs | 613 | | 347 | | 35,860 | 10,160 | −72 |
| OPFRs | TBP | 1.5 | ±0.3 | 0.8 | ±0.4 | 260 | 94 | −64 |
| | TCEP | 6.1 | ±1.9 | 2.1 | ±1.4 | 230 | 270 | 19 |
| | TCPP | 14 | ±16 | 20.5 | ±15 | 4,800 | 4,700 | −3.3 |
| | TDCP | 1.5 | ±0.5 | b.d.l. | | 129 | 187 | 45 |
| | TPhP | 7.2 | ±3.5 | b.d.l. | | 284 | 268 | −5.6 |
| | ΣOPFRs | 30.3 | | 23.4 | | 5,703 | 5,519 | −3.2 |

[a]*b.d.l. Below detection limit.*

similar to those described in Bosnia Herzegovina, 9.9 pg $m^{-3}$ (Lammel et al., 2011). The respective α- and γ-HCH concentrations, 3.5 and 12.9 pg $m^{-3}$ during B1 and 0.5 and 3.9 pg $m^{-3}$ during B2, were lower than those reported in other urban areas of Spain: 37 pg $m^{-3}$ for their sum (de la Torre et al., 2016).

The concentrations of total PCBs in B1 and B2, 58 and 23 pg $m^{-3}$, respectively (sum of congeners reported in **Table 2**), were again generally lower than those found in other urban areas from Italy: 117 pg $m^{-3}$ (Estellano et al., 2012), Spain: 122 pg $m^{-3}$ (Pozo et al., 2009), France: 3,100 pg $m^{-3}$ (Pozo et al., 2009), Turkey: 153–376 pg $m^{-3}$ (Kuzu, 2016), Argentina: 146–200 pg $m^{-3}$ (Tombesi et al., 2014; Astoviza et al., 2016), Chile: 160 pg $m^{-3}$ (Pozo et al., 2012), Canada: 481 pg $m^{-3}$ (Motelay-Massei et al., 2005), Pakistan: 37–293 pg $m^{-3}$ (Nasir et al., 2014), India: 278 pg $m^{-3}$ (Pozo et al., 2011), China: 600–7,600 pg $m^{-3}$ (Cui et al., 2017), and Bangladesh: 7–1,800 pg $m^{-3}$ (Nost et al., 2015). They were similar to those reported in Nepal: 1.2–47 pg $m^{-3}$ (Pokhrel et al., 2018).

Total PAHs in B1 and B2, approximately 36,000 and 10,000 pg $m^{-3}$, respectively (sum of the compounds reported in **Table 2**), were found in lower concentrations than those found in Strasbourg: 51,000 pg $m^{-3}$ (Morville et al., 2011) and Istanbul, 21,000–290,000 pg $m^{-3}$ (Kuzu, 2016) and higher than those found in the United States: 4,100–12,000 pg $m^{-3}$ (Pratt et al., 2018).

The concentrations of TBP in B1 and B2, 260 and 94 pg $m^{-3}$, were lower than those found in urban areas of Germany, 1,550 pg $m^{-3}$ (Zhou et al., 2017) and those of TCPP, 4,800 and 4,700 pg $m^{-3}$, respectively, were higher than those found in these urban areas, 2,700 pg $m^{-3}$ (Zhou et al., 2017). The concentrations of TDCP, 129 pg $m^{-3}$ in B1 and 187 pg $m^{-3}$ in B2, and of TPhP, 284 pg $m^{-3}$ in B1 and 268 pg $m^{-3}$ in B2, were higher than those reported in urban air in Sweden, 7.6 and 47 pg $m^{-3}$, respectively (Wong et al., 2018).

The concentrations of PCBs in Barcelona in the B1 period, 58 pg $m^{-3}$, were about four times higher than in the continental background station 14.6 pg $m^{-3}$ (**Table 2**), whereas those of PAHs, 36,000 pg $m^{-3}$, were about 60 times higher than in Aigüestortes, 613 pg $m^{-3}$, and those of the OPFRs were between 38 and 340 times higher (**Table 2**). The concentrations of HCHs were two to twelve times higher in Barcelona during the B1 period compared to the background location (**Table 2**). In contrast, HCB and PeCB in the continental background station were nearly two and three times higher than in the B1 period in Barcelona. The differences in PCB, HCB and PeCB air concentrations between

urban and remote sites compared to PAHs and OPFRs could be explained by fundamental differences in emission sources. The production and use of PCBs and most OCs have been restricted for several decades, but they are present in urban waste at low amounts (Wegiel et al., 2011; Neuwahl et al., 2019) which constitute a potential source in cities such as Barcelona. However, these legacy POPs may still be released to the atmosphere from diffusive secondary sources, including other environmental compartments (Grimalt et al., 2009), especially so in cold and remote areas that now might act as repositories for persistent contaminants such as HCB (Meijer et al., 2003). Contrarily, PAHs are still emitted from many primary combustion sources, such as traffic and domestic emissions in urban areas, while OPFRs are widely applied as flame retardants in construction material, household products and electronic equipment.

## Assessment of the Lockdown Changes on Airborne POPs and OPFRs

One of the main features of **Table 2** is the strong decrease of HCB and PeCB between B1 and B2 periods, −79 and −90.5%, respectively (**Table 2**). At present, the occurrence of these compounds in the atmosphere of urban areas without industrial activity is mainly related to waste treatment, including incineration (EPA, 1986; Martens et al., 1998; Bailey, 2001; Wegiel et al., 2011). The lockdown period in Barcelona involved a −24.6% reduction of urban waste generation (a reduction of almost 20,000 tons of solid waste) which, in turn, represented incineration decreases between −25 and −28% when quantified as $CO_2$ emission (Montlleo et al., 2020; State of the City, 2020). These reductions may have contributed to the decrease in the concentrations of these compounds. Other processes, e.g., less transport of materials, may also have been relevant for the observed decrease.

Polycyclic aromatic hydrocarbons also showed high reduction of atmospheric concentrations, between −68 and −87% (**Table 2**). Atmospheric PAHs in urban areas are primarily generated as by-products of motorized transport. Therefore, the observed differences are in agreement with the strong reduction of traffic in Barcelona, −80%, during the lockdown period (Montlleo et al., 2020; State of the City, 2020).

The atmospheric concentrations of PCBs and other OCs like the HCHs were also strongly depleted, between −34 and −69.5%, and between −70 and −86%, respectively. These decreases were probably related with the −24.6% reduction in waste generation during lockdown (Montlleo et al., 2020; State of the City, 2020) as incineration of urban waste is one main PCB source in the air of urban areas (Neuwahl et al., 2019; Arp et al., 2020) due to the presence of such compounds in urban waste and their high resistance to combustion (Neuwahl et al., 2019).

The OPFRs showed different trends (**Table 2**). TBP was the only compound following the concentration differences of OCs and PAHs, which were reflected in a large reduction in concentration, −64%, between the B1 and B2 periods. In contrast, the other OPFRs showed small decreases or even increases in atmospheric concentrations. This is probably related with the fundamentally different sources of OPFRs, e.g., being related with construction material, household products and electronic equipment over time, thus being less susceptible to variations in urban and industrial activities.

## Changes in Atmospheric Gases and Particles

The average concentrations of CO, $PM_{10}$, NO, and $NO_2$ in Barcelona in the B2 period of 2020 show lower values than those of the 2018–2019 average, whereas these differences are not observed for B1 (**Supplementary Figure 1**). Similarly, the concentrations of these gases and $PM_{10}$ in the lockdown period of 2020 are much lower than those in the equivalent time interval of the 2018–2019 average. This difference is the opposite in the case of $O_3$, which is consistent with the lack of NO during lockdown and higher insolation during spring months. An initial study encompassing the first lockdown weeks (March 14–March 30) showed consistent changes (Tobias et al., 2020). In the present study, comparison of the data encompassing

**TABLE 3 |** Results of the Bayesian model for the air pollutant concentrations in the pre-lockdown/lockdown and B1/B2 periods.

| Compound | Period | Average concentration | | | Effect of lockdown | | Causality | |
|---|---|---|---|---|---|---|---|---|
| | | Measured | Predicted ± SD | 95% CI | Effect ± SD | 95% CI | *p*-value | Probability (%) |
| CO (mg $m^{-3}$) | Pre/lock | 0.22 | 0.30 ±0.02 | [0.26, 0.34] | −28% ± 6.4% | [−40%, −16%] | 0.0011 | 99.89 |
| | B1/B2 | 0.25 | 0.37 ± 0.02 | [0.33, 0.41] | −32% ± 5.4% | [−43%, −22%] | 0.0011 | 99.89 |
| $PM_{10}$ (μg $m^{-3}$) | Pre/lock | 19 | 31 ± 2.2 | [26, 35] | −37% ± 7% | [−50%, −23%] | 0.0011 | 99.89 |
| | B1/B2 | 24 | 30 ± 1.8 | [27, 34] | −20% ± 5.9% | [−32%, −8.8%] | 0.0010 | 99.90 |
| NO (μg $m^{-3}$) | Pre/lock | 7.4 | 31 ± 4.3 | [23, 40] | −76% ± 14% | [−103%, −51%] | 0.0011 | 99.89 |
| | B1/B2 | 18 | 31 ± 4.1 | [23, 39] | −41% ± 13% | [−66%, −14%] | 0.0033 | 99.67 |
| $NO_2$ (μg $m^{-3}$) | Pre/lock | 22 | 47 ± 2.0 | [43, 51] | −52% ± 4.2% | [−61%, −44%] | 0.0011 | 99.89 |
| | B1/B2 | 33 | 52 ± 1.8 | [49, 56] | −38% ± 3.4% | [−44%, −31%] | 0.0012 | 99.88 |
| $O_3$ (μg $m^{-3}$) | Pre/lock | 56 | 38 ± 2.9 | [33, 44] | 45% ± 7.4% | [31%, 59%] | 0.0010 | 99.90 |
| | B1/B2 | 45 | 45 ± 3.0 | [39, 51] | −0.12% ±6.7% | [−13%, 12%] | 0.4985 | 50.00 |

*The average concentrations measured during the periods after lockdown restrictions (i.e., lockdown and B2) are compared to the concentrations (± standard deviation, SD) predicted by the model from data including the two previous years. Confidence intervals (95%), p-values, and probability of the observed concentration changes caused by lockdown measures are provided.*

the whole lockdown period using a Bayesian structured time-series model (CausalImpact 1.2.4 R package, Brodersen et al., 2015) also allowed to account for the influence of seasonal effects on the concentration changes. Accordingly, the pollutant concentrations of 2020 were used as the response series and the average pollutant data of 2018–2019 as the control series, which was assumed not affected by the lockdown measures, consistently with the absence of restrictions in 2018–2019. The applicability of this model to these data was supported by comparison of the time series and dummy causal impact analyses performed with imaginary intervention periods which provided reasonable predictions and low causality probabilities.

The Bayesian analysis of the whole lockdown period showed noticeable concentration reductions of CO, NO, and $NO_2$ coinciding with the lockdown measures of March 2020, which picked up slightly after lockdown easing at the end of May 2020 and finally returned to ordinary levels at the end of lockdown (**Figure 1**). The same representations showing the predictions calculated for the B1/B2 sampling periods can be found in **Supplementary Figure 2**. The causal impact analysis of CO, NO, and $NO_2$ concentrations for the pre-lockdown/lockdown periods yielded statistically significant average variations of −28, −76, and −52%, respectively ($p$ = 0.0011; **Table 3**). Despite the B2 sampling period included some weeks before and after lockdown, similar (−32% CO) or slightly lower (−41% NO, −38% $NO_2$) but still significant reductions were observed for the same compounds, $p$ = 0.0011, 0.0033, and 0.0012, respectively (**Table 3**). These differences indicated a direct influence of lockdown restrictions as consequence of the steep decline in motor vehicle traffic, the main contributing source of CO and NO through direct emissions (EEA, 2019) as well as $NO_2$ formation by reaction of NO with atmospheric $O_3$.

The decrease between the usual polluting conditions and the lockdown period is more intense in areas with a lot of traffic such as downtown Barcelona, although it is also noticeable in the north and west forested areas, as shown in **Figure 2** where the atmospheric $NO_2$ concentrations are displayed for the B1, B2, and specific lockdown periods. Comparison of the average $NO_2$ concentrations in the B2 and specific lockdown periods from this figure shows very similar distributions which support the representativeness of the sampled B2 interval concerning lockdown conditions.

Reductions in NO concentrations usually lead to increasing $O_3$ concentrations (Leighton, 1961), which are also observed in **Figure 1**. However, $O_3$ levels usually increase in the months leading up to the summer (with higher temperatures and increased solar radiation), which can lead to misidentification of an effect of lockdown on $O_3$ concentrations. The Bayesian time-series prediction model used here corrects for seasonal effects by taking into account data from the previous 2 years and shows a statistically significant increase of $O_3$ concentrations in the lockdown period (+45%; $p$ = 0.001) which overcomes these effects. The increases in $O_3$ during the B2 and lockdown periods are also documented in **Figure 2**. In this case, the increases in $O_3$ are greater in the forested areas because downtown the NO from traffic still decreases the concentrations of this oxidant. Again, the differences between the B2 and lockdown periods are small.

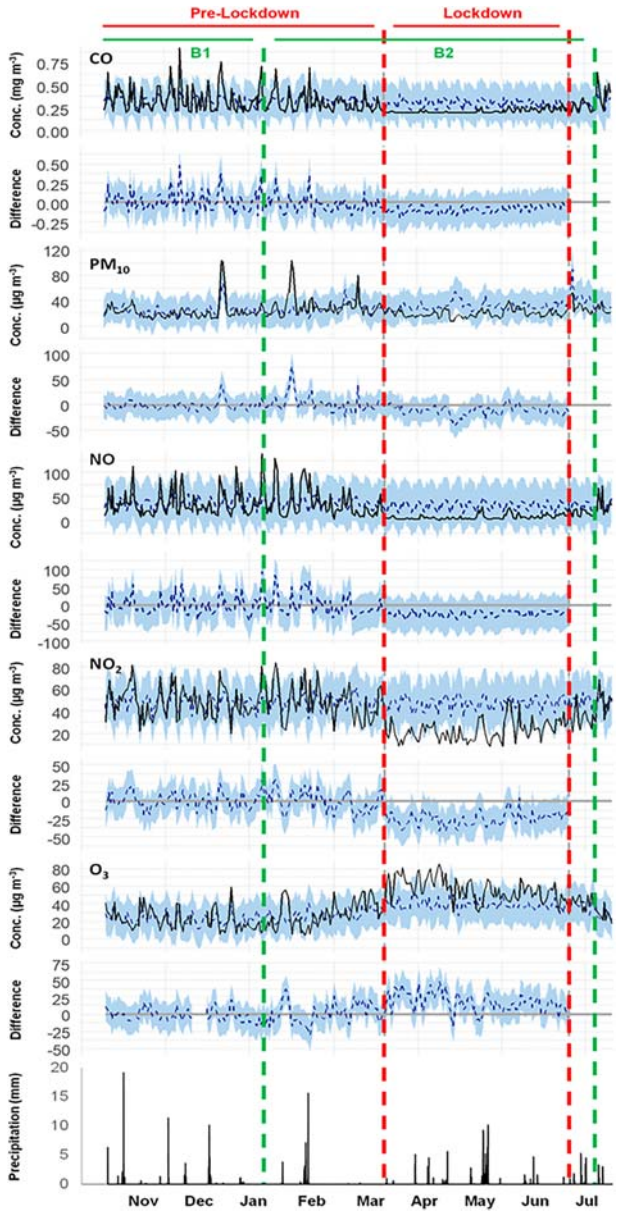


**FIGURE 1 |** Representation of the concentrations of atmospheric pollutants in Barcelona during the lockdown of 2020 and the corresponding Bayesian model predictions. The pre-lockdown/lockdown and the PAS-sampled B1/B2 periods are delimited by dashed, vertical, red and green lines, respectively. For each compound, the top graphs show daily average concentrations recorded in 2020 (black continuous line) against a counterfactual prediction based on 2018–2019 average values (blue dashed line). The bottom graphs show the difference between the observed data and the counterfactual predictions if lockdown had not occurred. From data of the air monitoring stations of the Catalan Government.

Concerning $PM_{10}$, the concentration decrease was noticed both for the lockdown (−37%; $p$ = 0.0011) and the B2 periods (−20%; $p$ = 0.001). This change is small in comparison with those observed for the gases except in the case of CO, which suggest that besides traffic other

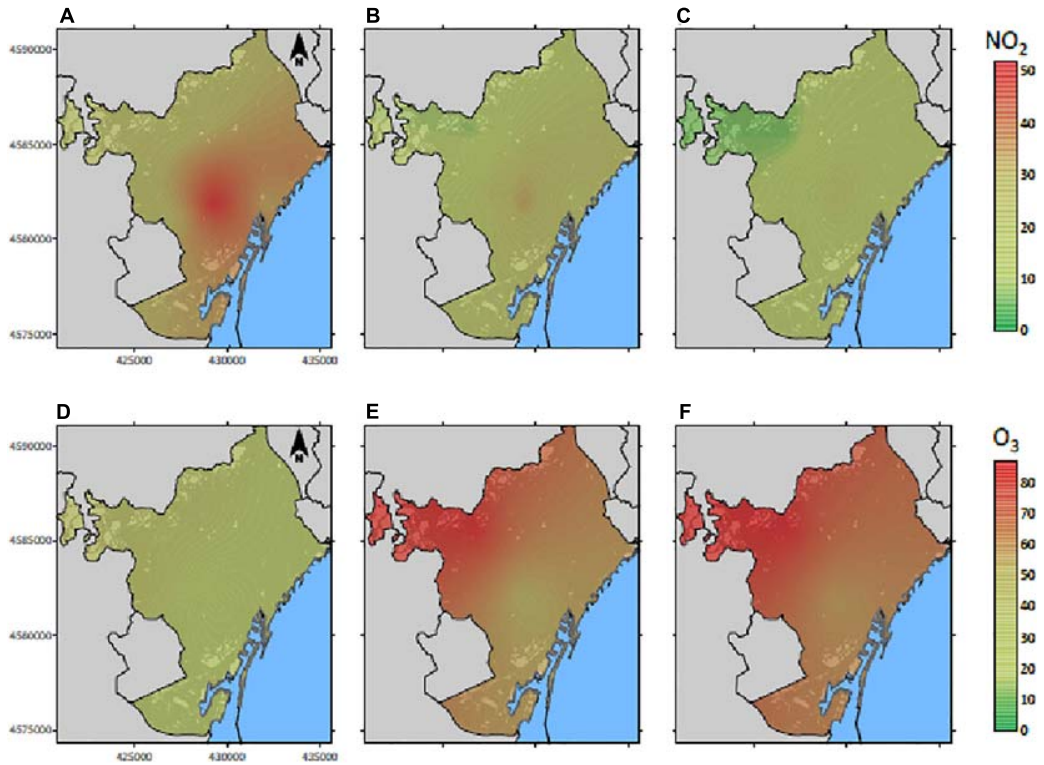


**FIGURE 2 |** Spatial distributions of airborne $NO_2$ **(A–C)** and $O_3$ **(D–F)** Barcelona, averaging in the B1 [15 October 2019–9 January 2020; **(A,D)**], B2 [9 January 2020–15 July 2020; **(B,E)]** and specific lockdown [15 March 2020–22 June 2020; **(C,F)**] periods. The plotted values ($\mu g\ m^{-3}$) are the averages of the daily measurements between 7 and 20 h. Note that the north and west zones are forested. From data of the air monitoring stations of the Catalan Government.

sources contributed to the atmospheric concentrations of $PM_{10}$ in the city.

These results are in the range of those reported in other studies from several European and Mediterranean urban areas that also experienced lockdown conditions during the first half of 2020. Other studies in the city of Barcelona reported $NO_2$ reductions in concentration of −50% (Baldasano, 2020), −47 to −61% (Petetin et al., 2020), and −51% (Tobias et al., 2020). These values are similar to those reported in Madrid, −39 to −59% (Petetin et al., 2020), −62% (Baldasano, 2020), and −35 to −50% (Shi et al., 2021), and also to the average meteorology-normalized Spanish average of −50% (Petetin et al., 2020). Other European cities also presented comparable $NO_2$ reductions like −61% in Milan (Collivignarelli et al., 2020), −39% in Lucca and −39% in Florence (Donzelli et al., 2020), −32% in Athens (Grivas et al., 2020), and somewhat larger than −16, −27, −8, −26, and −11% in Milan, Rome, London, Paris, and Berlin, respectively (Shi et al., 2021). Our results for other pollutants are also similar to those reported for $PM_{10}$: −31% in Barcelona (Tobias et al., 2020), −48% in Milan (Collivignarelli et al., 2020), and −31% in Florence (Donzelli et al., 2020); for CO: −58% in Milan (Collivignarelli et al., 2020) and −35% in Athens (Grivas et al., 2020); and for NO: −42% in Pisa (Donzelli et al., 2020). Finally, compared to our results, other reports show similar $O_3$ variations in Barcelona: +33% increase during the first lockdown weeks (Tobias et al., 2020); slightly lower variations of −2% to +30% in several European cities (Shi et al., 2021); and much higher variations of +252% in Milan (Collivignarelli et al., 2020).

Moreover, air pollutant concentration reductions over the first weeks of lockdown have also been reported in a broader scale through satellite imaging techniques. The European Space Agency reported central and southern European reductions of $NO_2$ concentrations in Madrid (−48%), Rome (−49%), Milan (−47%), and Paris (−54%) (ESA, 2020a,b). These values are well in agreement with the values summarized in the paragraph above, as well as in the range of those reported here for the city of Barcelona (**Table 3**).

Finally, daily precipitation episodes are also represented in **Figure 1**. Comparison with the daily concentrations of all gases (i.e., CO, NO, $NO_2$, and $O_3$) and $PM_{10}$ evidences that rain events generally do not coincide with noticeable drops in their atmospheric concentrations. This is consistent with results presented by other studies assessing changes in air pollution during lockdown in several cities in Spain, which found no correlation between precipitation values and air pollutant concentrations (Briz-Redón et al., 2021). Contrarily, the overall trend in concentration differences was consistent with the lockdown period, leaving wet precipitation as a minor driving factor in reducing air pollutant concentrations. This observation can be extrapolated to the atmospheric POP distributions. Rainfall rates averaged by sampled time can be derived from **Table 1** and are sufficiently similar for both PAS-sampled periods

(2.6 and 2.7 mm $day^{-1}$ for B1 and B2, respectively) as to not expect considerable differences in washout, leaving the lockdown as the main cause for pollutant reductions.

## CONCLUSION

All examined airborne pollutants showed lower concentrations during lockdown than in the regular period. PeCB was the compound displaying the highest lockdown decrease, −90.5%, followed by HCB and some PAHs such as b[a]ant and pyr, −79, −87, and −81%, respectively. In general, PAHs were the pollutants with higher reduction, −68 to −87%. Other compounds such as PCBs decreased by −37 to −69.5%.

The drops in atmospheric PAH concentrations can be associated with the strong traffic decrease during lockdown, −80% on average, and the significant reduction of harbor activities in this time interval, in the order of −65%. The present results regarding atmospheric PAHs indicate that the observed improvement of urban atmospheric quality related with lockdown restrictions was even better than recorded in the changes of nitrogen oxides and CO, providing a more holistic approach.

The study of other pollutants such as HCB, PeCB, and PCBs also evidences other atmospheric improvements related with the lockdown period such as the beneficial effects of reduction in the generation of solid residues and the subsequent reduction of urban waste incineration. The concentrations of PCBs during the B2 period in Barcelona were very close to those of remote sites such as the Pyrenees, with HCB and PeCB showing lower levels than those in these remote areas even during the pre-lockdown period.

Concerning the OPFRs, TBP also showed a decrease during lockdown but the other compounds of this group were seemingly not affected by the restrictions, possibly as a result of distinct and uniform release from their emission sources, e.g., construction material, industrial applications, household products, and others.

All in all, a significant decrease on the gas phase concentrations of atmospheric pollutants with current sources linked with anthropogenic urban activity was observed as consequence of the lockdown restrictions. $O_3$ is an exception related to processes other than traffic. The present work evidences the effectiveness of reducing overall anthropogenic emissions on a relatively short time span, not only in air quality indicator pollutants but also in many POPs. This highlights the potential of much needed policies that tackle air quality in a more stringent and broader way, which should stem from reports like the one we present. A sustained improvement on air quality, especially in densely populated areas, would contribute to reduce the over four million deaths attributed every year to ambient air pollution (WHO, 2018), as well as improve the health of many more.

## DATA AVAILABILITY STATEMENT

The raw data supporting the conclusions of this article will be made available by the authors, without undue reservation.

## AUTHOR CONTRIBUTIONS

RP: sampling, analysis, formal analysis, visualization, and writing – original draft. BD: sampling, analysis, supervision, and writing – review and editing. PF: supervision, writing – review and editing. EM: Formal analysis and visualization. JG: conceptualization, writing – review and editing, and funding acquisition. All authors contributed to the article and approved the submitted version.

## FUNDING

This work was supported by the Spanish Ministry of Science and Innovation (Projects: CUANTOX CTM2015-71832-P and INTEMPOL PGC2018-10228-B-I00). RP also acknowledges financial support from the Spanish Ministry of Science and Innovation (BES-2016-076339).

## ACKNOWLEDGMENTS

Sampling support from Alejandro G. Inarra and Anna Canals-Angerri, and technical assistance from Roser Chaler are acknowledged. Part of this work was performed in the Parc Nacional d'Aigüestortes i Estany de Sant Maurici, in Catalonia, with collaboration from the Department of Territory and Sustainability of the Catalan Government.

## SUPPLEMENTARY MATERIAL

The Supplementary Material for this article can be found online at: https://www.frontiersin.org/articles/10.3389/fenvs.2021.650539/full#supplementary-material

## REFERENCES

Armstrong, B., Hutchinson, E., Unwin, J., and Fletcher, T. (2004). Lung cancer risk after exposure to polycyclic aromatic hydrocarbons: a review and meta-analysis. *Environ. Health Perspect.* 112, 970–978. doi: 10.1289/ehp.6895

Arp, H. P. H., Morin, N. A. O., Andersson, P. L., Hale, S. E., Wania, F., Breivik, K., et al. (2020). The presence, emission and partitioning behavior of polychlorinated biphenyls in waste, leachate and aerosols from Norwegian waste-handling facilities. *Sci. Total Environ.* 715:136824. doi: 10.1016/j.scitotenv.2020.136824

Astoviza, M. J., Cappelletti, N., Bilos, C., Migoya, M. C., and Colombo, J. C. (2016). Airborne PCB patterns and urban scale in the Southern Río de la Plata Basin, Argentina. *Sci. Total Environ.* 572, 16–22. doi: 10.1016/j.scitotenv.2016.07.101

Baek, S. O., Field, R. A., Goldstone, M. E., Kirk, P. W., Lester, J. N., and Perry, R. (1991). A review of atmospheric polycyclic hydrocarbons: sources, fate and behavior. *Water Air Soil Pollut.* 60, 279–300. doi: 10.1007/BF00282628

Bailey, R. E. (2001). Global hexachlorobenzene emissions. *Chemosphere* 43, 167–182. doi: 10.1016/S0045-6535(00)00186-7

Baldasano, J. M. (2020). COVID-19 lockdown effects on air quality by NO2 in the cities of Barcelona and Madrid (Spain). *Sci. Total Environ.* 741:140353. doi: 10.1016/j.scitotenv.2020.140353

Berman, J. D., and Ebisu, K. (2020). Changes in U.S. air pollution during the COVID-19 pandemic. *Sci. Total Environ.* 739:139864. doi: 10.1016/j.scitotenv.2020.139864

Boström, C. E., Gerde, P., Hanberg, A., Jernström, B., Johansson, C., Kyrklund, T., et al. (2002). Cancer risk assessment, indicators, and guidelines for polycyclic aromatic hydrocarbons in the ambient air. *Environ. Health Perspect.* 110, 451–488. doi: 10.1289/ehp.110-1241197

Brodersen, K. H., Galluser, F., Koehler, J., Remy, N., and Scott, S. L. (2015). *CausalImpact 1.2.4. Ann. Appl. Stat*. Available online at: http://google.github.io/CausalImpact/ (accessed October 15, 2020).

Briz-Redón, Á, Belenguer-Sapiña, C., and Serrano-Aroca, Á (2021). Changes in air pollution during COVID-19 lockdown in Spain: a multi-city study. *J. Environ. Sci.* 101, 16–26. doi: 10.1016/j.jes.2020.07.029

Cameletti, M. (2020). The effect of corona virus lockdown on air pollution: evidence from the city of Brescia in Lombardia Region (Italy). *Atmos. Environ.* 239:117794. doi: 10.1016/j.atmosenv.2020.117794

Casas, M., Nieuwenhuijsen, M., Martinez, D., Ballester, F., Basagaña, X., Barterrechea, M., et al. (2015). Prenatal exposure to PCB-153, p,p'-DDE and birth outcomes in 9000 mother-child pairs: Exposure-response relationship and effect modifiers. *Environ. Int.* 74, 23–31. doi: 10.1016/j.envint.2014.09.013

Chakraborty, P., Zhang, G., Li, J., Xu, Y., Liu, X., Tanabe, S., et al. (2010). Selected organochlorine pesticides in the atmosphere of major Indian cities: levels, regional versus local variations, and sources. *Environ. Sci. Technol.* 44, 8038–8043. doi: 10.1021/es102029t

Chen, Y., Cai, X., Jiang, L., and Li, Y. (2016). Prediction of octanol-air partition coefficients for polychlorinated biphenyls (PCBs) using 3D-QSAR models. *Ecotoxicol. Environ. Saf.* 124, 202–212. doi: 10.1016/j.ecoenv.2015.10.024

Chevrier, J., Eskenazi, B., Holland, N., Bradman, A., and Barr, D. B. (2008). Effects of exposure to polychlorinated biphenyls and organochlorine pesticides on thyroid function during pregnancy. *Am. J. Epidemiol.* 168, 298–310. doi: 10.1093/aje/kwn136

Collivignarelli, M. C., Abbà, A., Bertanza, G., Pedrazzani, R., Ricciardi, P., and Miino, M. C. (2020). Lockdown for CoViD-2019 in Milan: what are the effects on air quality? *Sci. Total Environ.* 732:139280. doi: 10.1016/j.scitotenv.2020.139280

Cui, S., Fu, Q., Li, Y.-F., Li, T.-X., Liu, D., Dong, W.-C., et al. (2017). Spatial–temporal variations, possible sources and soil–air exchange of polychlorinated biphenyls in urban environments in China. *RSC Adv.* 7:14797. doi: 10.1039/C6RA26864A

de la Torre, A., Sanz, P., Navarro, I., and Martínez, M. A. (2016). Time trends of persistent organic pollutants in Spanish air. *Environ. Pollut.* 217, 26–32. doi: 10.1016/j.envpol.2016.01.040

De Voogt, P., Wells, D. E., Reutergardh, L., and Brinkman, U. A. T. (1990). Biological activity, determination and occurrence of planar, mono- and di-ortho PCBs. *Int. J. Environ. Anal. Chem.* 40, 1–46. doi: 10.1080/03067319008030516

Dishaw, L. V., Powers, C. M., Ryde, I. T., Roberts, S. C., Seidler, F. J., Slotkin, T. A., et al. (2011). Is the PentaBDE replacement, tris (1,3-dichloro-2-propyl) phosphate (TDCPP), a developmental neurotoxicant? Studies in PC12 cells. *Toxicol. Appl. Pharmacol.* 256, 281–289. doi: 10.1016/j.taap.2011.01.005

Donzelli, G., Cioni, L., Cancellieri, M., Morales, A. L., and Suárez-Varela, M. M. M. (2020). The Effect of the Covid-19 lockdown on air quality in three Italian medium-sized cities. *Atmosphere* 11:1118. doi: 10.3390/atmos11101118

Du, J., Li, H., Xu, S., Zhou, Q., Jin, M., and Tang, J. (2019). A review of organophosphorus flame retardants (OPFRs): occurrence, bioaccumulation, toxicity, and organism exposure. *Environ. Sci. Pollut. Res.* 26, 22126–22136. doi: 10.1007/s11356-019-05669-y

EEA (2019). *Air Quality in Europe – EEA Report No 10/2019*. Available online at: https://www.eea.europa.eu/publications/air-quality-in-europe-2019 (accessed November 15, 2020).

EPA (1986). *Exposure Assessment for Hexachlorobenzene*. Washington, DC: U.S. Environmental Protection Agency, Office of Pesticides and Toxic Substances.

ESA (2020a). *Nitrogen Dioxide Concentrations Over Spain*. Available online at: http://www.esa.int/ESA_Multimedia/Images/2020/03/Nitrogen_dioxide_concentrations_over_Spain (accessed November 15, 2020).

ESA (2020b). *Air Pollution Remains Low as Europeans Stay at Home*. Available online at: http://www.esa.int/Applications/Observing_the_Earth/Copernicus/Sentinel-5P/Air_pollution_remains_low_as_Europeans_stay_at_home (accessed November 15, 2020).

Estellano, V. H., Pozo, K., Harner, T., Carsolini, S., and Focardi, S. (2012). Using PUF disk passive samplers to simultaneously measure air concentrations of persistent organic pollutants (POPs) across the Tuscany Region, Italy. Atmos. *Pollut. Res.* 3, 88–94. doi: 10.5094/APR.2012.008

Grandjean, P., and Landrigan, P. J. (2014). Neurobehavioural effects of developmental toxicity. *Lancet Neurol.* 13, 330–338. doi: 10.1016/S1474-4422(13)70278-3

Grimalt, J. O., Sunyer, J., Moreno, V., Amaral, O. C., Sala, M., Rosell, A., et al. (1994). Risk excess of soft−tissue sarcoma and thyroid cancer in a community exposed to airborne organochlorinated compound mixtures with a high hexachlorobenzene content. *Int. J. Cancer.* 56, 200–203. doi: 10.1002/ijc.2910560209

Grimalt, J. O., Fernandez, P., and Quiroz, R. (2009). Input of organochlorine compounds by snow to European high mountain lakes. *Freshwater Biol.* 54, 2533–2542. doi: 10.1111/j.1365-2427.2009.02302.x

Grivas, G., Athanasopoulou, E., Kakouri, A., Bailey, J., Liakakou, E., Stavroulas, I., et al. (2020). Integrating in situ measurements and city scale modelling to assess the COVID-19 lockdown effects on emissions and air quality in Athens, Greece. *Atmosphere* 11:1174. doi: 10.3390/atmos11111174

Harner, T., Su, K., Genualdi, S., Karpowicz, J., Ahrens, L., Mihele, C., et al. (2013). Calibration and application of PUF disk passive air samplers for tracking polycyclic aromatic compounds (PACs). *Atmos. Environ.* 75, 123–128. doi: 10.1016/j.atmosenv.2013.04.012

Harner, T. (2016). 2016 v1 3 Template for Calculating PUF and SIP Disk Sample Air Volumes. doi: 10.13140/RG.2.1.3998.8884

He, J., and Balasubramanian, R. (2012). Passive sampling of gaseous persistent organic pollutants in the atmosphere. *Energy Proc.* 16, 494–500. doi: 10.1016/j.egypro.2012.01.080

Kalina, J., White, K. B., Scheringer, M., Pøibylová, P., Kukuèka, P., Audy, O., et al. (2019). Comparability of long-term temporal trends of POPs from co-located active and passive air monitoring networks in Europe. *Environ. Sci. Processes Impacts* 21, 1132–1142. doi: 10.1039/C9EM00136K

Kaufman, Y. J., Tanré, D., Remer, L. A., Vermote, E. F., Chu, A., and Holben, B. N. (1997). Operational remote sensing of tropospheric aerosol over land from EOS moderate resolution imaging spectroradiometer. *J. Geophys. Res. Atmos.* 102, 17051–17067. doi: 10.1029/96jd03988

Krotkov, N. A., McLinden, C. A., Li, C., Lamsal, L. N., Celarier, E. A., Marchenko, S. V., et al. (2016). Aura OMI observations of regional SO2 and NO2 pollution changes from 2005 to 2015. *Atmos. Chem. Phys.* 16, 4605–4629. doi: 10.5194/acp-16-4605-2016

Kuzu, S. L. (2016). Compositional variation of PCBs, PAHs, and OCPs at Gas phase and size segregated particle phase during dust incursion from the Saharan desert in the Northwestern Anatolian peninsula. *Adv. Meteorol.* 2016:7153286. doi: 10.1155/2016/7153286

Lammel, G., Klanova, J., Eric, L., Ilic, P., Kohoutek, J., and Kovacik, I. (2011). Sources of organochlorine pesticides in air in an urban Mediterranean environment: volatilization from soil. *J. Environ. Monit.* 13, 3358–3364. doi: 10.1039/C1EM10479A

Lauby-Secretan, B., Loomis, D., Grosse, Y., El Ghissassi, F., Bouvard, V., Benbrahim-Tallaa, L., et al. (2013). Carcinogenicity of polychlorinated biphenyls and polybrominated biphenyls. *Lancet Oncol.* 14, 287–288. doi: 10.1016/S1470-2045(13)70104-9

Le Quéré, C., Jackson, R. B., Jones, M. W., Smith, A. J. P., Abernethy, S., Andrew, R. M., et al. (2020). Temporary reduction in daily global CO2 emissions during the COVID-19 forced confinement. *Nat. Clim. Chang.* 10, 647–653. doi: 10.1038/s41558-020-0797-x

Leighton, P. A. (1961). *Photochemistry of Air Pollution*. New York, NY: Academic Press.

Li, L., Li, Q., Huang, L., Wang, Q., Zhu, A., Xu, J., et al. (2020). Air quality changes during the COVID-19 lockdown over the Yangtze River Delta Region: an insight into the impact of human activity pattern changes on air pollution variation. *Sci. Total Environ.* 732:139282. doi: 10.1016/j.scitotenv.2020.139282

Liu, D., Lin, T., Shen, K., Li, J., Yu, Z., and Zhang, G. (2016). Occurrence and concentrations of halogenated flame retardants in the atmospheric fine particles in Chinese cities. *Environ. Sci. Technol.* 50, 9846–9854. doi: 10.1021/acs.est.6b01685

Llop, S., Murcia, M., Alvarez-Pedrerol, M., Grimalt, J. O., Santa Marina, L., Julvez, J., et al. (2017). Association between exposure to organochlorine compounds

and maternal thyroid status: Role of the iodothyronine deiodinase 1 gene. *Environ. Int.* 104, 83–90. doi: 10.1016/j.envint.2016.12.013

Lopez-Espinosa, M. J., Murcia, M., Iniguez, C., Vizcaíno, E., Costa, O., Fernández-Somoano, A., et al. (2016). Organochlorine compounds and ultrasound measurements of fetal growth in the INMA Cohort (Spain). *Environ. Health Perspect.* 124, 157–163. doi: 10.1289/ehp.1408907

Martens, D., Balta-Brouma, K., Brotsack, R., Michalke, B., Schramel, P., Klimm, C., et al. (1998). Chemical impact of uncontrolled solid waste combustion to the vicinity of the Kouroupitos Ravine, Crete, Greece. *Chemosphere* 36, 2855–2866. doi: 10.1016/S0045-6535(97)10242-9

Meijer, S. N., Ockenden, W. A., Sweetman, A., Breivik, K., Grimalt, J. O., and Jones, K. C. (2003). Global distribution and budget of PCBs and HCB in Background surface soils: implications for sources and environmental processes. *Environ. Sci. Technol.* 37, 667–672. doi: 10.1021/es010322i

Montlleo, M., Rodriguez, G., Tavares, N., Masvidal, M., Lao, J., Coral, A., et al. (2020). *Observatori COVID-19. Metabolisme de la Ciutat. City Hall of Barcelona*. Available online at: https://www.barcelona.cat/barcelona-pel-clima/sites/default/files/documents/20200729-observatori_covid-19-metabolisme_de_la_ciutat.pdf (accessed November 15, 2020).

Morales, E., Gascon, M., Martinez, D., Casas, M., Ballester, F., Rodriguez-Bernal, C. L., et al. (2013). Associations between blood persistent organic pollutants and 25-hydroxyvitamin D3 in pregnancy. *Environ. Int.* 57–58, 34–41. doi: 10.1016/j.envint.2013.03.011

Morville, S., Delhomme, O., and Millet, M. (2011). Seasonal and diurnal variations of atmospheric PAH concentrations between rural, suburban and urban areas. *Atmos. Pollut. Res.* 2, 366–373. doi: 10.5094/APR.2011.041

Motelay-Massei, A., Harner, T., Shoeib, M., Diamond, M., Stern, G., and Rosenbreg, B. (2005). Using passive air samplers to assess urban-rural trends for persistent organic pollutants and polycyclic aromatic hydrocarbons. 2. Seasonal trends for PAHs, PCBs, and organochlorine pesticides. *Environ. Sci. Technol.* 39, 5763–5773. doi: 10.1021/es0504183

Nasir, J., Wang, X., Xu, B., Wang, C., Joswiak, D. R., Rehman, S., et al. (2014). Selected organochlorine pesticides and polychlorinated biphenyls in urban atmosphere of Pakistan: concentration, spatial variation and sources. *Environ. Sci. Technol.* 48, 2610–2618. doi: 10.1021/es404711n

Neuwahl, F., Cusano, G., Gomez-Benavides, J., Holbrook, S., and Roudier, S. (2019). *Best Available Techniques (BAT). Reference Document for waste incineration. Industrial Emission Directive 2010/75/EU. Integrated Pollution Prevention and Control*. Luxembourg: Publications Office of the European Union.

Nost, T. H., Halse, A. K., Randall, S., Borgen, A. R., Schlabach, M., Paul, A., et al. (2015). High concentrations of organic contaminants in air from ship breaking activities in Chittagong, Bangladesh. *Environ. Sci. Technol.* 49, 11372–11380. doi: 10.1021/acs.est.5b03073

Odabasi, M., Cetin, E., and Sofuoglu, A. (2006). Determination of octanol-air partition coefficients and supercooled liquid vapor pressures of PAHs as a function of temperature: Application to gas-particle partitioning in an urban atmosphere. *Atmos. Environ.* 40, 6615–6625. doi: 10.1016/j.atmosenv.2006.05.051

Petetin, H., Bowdalo, D., Soret, A., Guevara, M., Jorba, O., Serradell, K., et al. (2020). Meteorology-normalized impact of the COVID-19 lockdown upon NO2 pollution in Spain. *Atmos. Chem. Phys.* 20, 11119–11141. doi: 10.5194/acp-20-11119-2020

Pokhrel, B., Gong, P., Wang, X., Khanal, S. N., Ren, J., Wang, C., et al. (2018). Atmospheric organochlorine pesticides and polychlorinated biphenyls in urban areas of Nepal: spatial variation, sources, temporal trends, and long-range transport potential. *Atmos. Chem. Phys.* 18, 1325–1336. doi: 10.5194/acp-18-1325-2018

Pozo, K., Harner, T., Lee, S. C., Wania, F., Muir, D. C. G., and Jones, K. C. (2009). Seasonally resolved concentrations of persistent organic pollutants in the global atmosphere from the first year of the GAPS Study. *Environ. Sci. Technol.* 43, 796–803. doi: 10.1021/es802106a

Pozo, K., Harner, T., Lee, S. C., Sinha, R. K., Sengupta, B., Loewen, M., et al. (2011). Assessing seasonal and spatial trends of persistent organic pollutants (POPs) in Indian agricultural regions using PUF disk passive air samplers. *Environ. Pollut.* 159, 646–653. doi: 10.1016/j.envpol.2010.09.025

Pozo, K., Harner, T., Rudolph, A., Oyola, G., Estellano, V. H., Ahumada-Rudolph, R., et al. (2012). Survey of persistent organic pollutants (POPs) and polycyclic aromatic hydrocarbons (PAHs) in the atmosphere of rural, urban and industrial areas of Concepciün, Chile, using passive air samplers. *Atmos. Poll. Res.* 3, 426–434. doi: 10.5094/APR.2012.049

Pratt, G. C., Herbrandson, C., Krause, M. J., Schmitt, C., Lippert, C. J., McMahon, C. R., et al. (2018). Measurements of gas and particle polycyclic aromatic hydrocarbons (PAHs) in air at urban, rural and near-roadway sites. *Atmos. Environ.* 179, 268–278. doi: 10.1016/j.atmosenv.2018.02.035

Sala, M., Sunyer, J., Herrero, C., To-Figueras, J., and Grimalt, J. O. (2001). Association between serum concentration of hexachlorobenzene and polychlorobiphenyls with thyroid hormone and liver enzymes in a sample of the general population. *Occup. Environ. Med.* 58, 172–177. doi: 10.1136/oem.58.3.172

Salamova, A., Hermanson, M. H., and Hites, R. A. (2014). Organophosphate and halogenated flame retardants in atmospheric particles from a European Arctic site. *Environ. Sci. Technol.* 48, 6133–6140. doi: 10.1021/es500911d

Shi, Z., Song, C., Liu, B., Lu, G., Xu, J., Vu, T. V., et al. (2021). Abrupt but smaller than expected changes in surface air quality attributable to COVID-19 lockdowns. *Sci. Adv.* 7:eabd6696. doi: 10.1126/sciadv.abd6696

Shoeib, M., and Harner, T. (2002). Characterization and comparison of three passive air samplers for persistent organic pollutants. *Environ. Sci. Technol.* 36, 4142–4151. doi: 10.1021/es020635t

Smink, A., Ribas-Fito, N., Garcia, R., Torrent, M., Mendez, M. A., Grimalt, J. O., et al. (2008). Exposure to hexachlorobenzene during pregnancy increases the risk of overweight in children aged 6 years. *Acta Paediatr.* 97, 1465–1469. doi: 10.1111/j.1651-2227.2008.00937.x

Sohrabi, C., Alsafi, Z., O'Neill, N., Khan, M., Kerwan, A., Al-Jabir, A., et al. (2020). World Health Organization declares global emergency: A review of the 2019 novel coronavirus (COVID-19). *Int. J. Surg.* 76, 71–76. doi: 10.1016/j.ijsu.2020.02.034

State of the City (2020). *State of the City. Barcelona City Hall Report. 2020*. Available online at: https://ajuntament.barcelona.cat/premsa/wp-content/uploads/2020/06/200626-Informe-Estat-de-la-ciutat-2019-Document-complementari.pdf (accessed November 15, 2020).

Tobias, A., Carnerero, C., Reche, C., Massagué, J., Via, M., Minguillón, M. C., et al. (2020). Changes in air quality during the lockdown in Barcelona (Spain) one month into the SARS-CoV-2 epidemic. *Sci. Total Environ.* 726:138540. doi: 10.1016/j.scitotenv.2020.138540

Tombesi, N., Pozo, K., and Harner, T. (2014). Persistent organic pollutants (POPs) in the atmosphere of agricultural and urban areas in the Province of Buenos Aires in Argentina using PUF disk passive air samplers. *Atmos. Pollut. Res.* 5, 170–178. doi: 10.5094/APR.2014.021

UNEP (2010). *United Nations Environment Programme. Assessing the Environmental Impacts of Consumption and Production. Priority Products and Materials*. Nairobi: UNEP.

Valvi, D., Mendez, M. A., Martinez, D., Grimalt, J. O., Torrent, M., Sunyer, J., et al. (2012). Prenatal concentrations of polychlorinated biphenyls, DDE, and DDT and overweight in children. A prospective birth cohort study. *Environ. Health Persp.* 120, 451–457. doi: 10.1289/ehp.1103862

Valvi, D., Mendez, M. A., Garcia-Esteban, R., Ballester, F., Ibarluzea, J., Goñi, F., et al. (2014). Prenatal exposure to persistent organic pollutants and rapid weight gain and overweight in infancy. *Obesity* 22, 488–496. doi: 10.1002/oby.20603

Van der Veen, I., and de Boer, J. (2012). Phosphorus flame retardants: Properties, production, environmental occurrence, toxicity and analysis. *Chemosphere* 88, 1119–1153. doi: 10.1016/j.chemosphere.2012.03.067

van Drooge, B. L., Grimalt, J. O., Camarero, L., Catalan, J., Stuchlík, E., and Torres García, C. J. (2004). Atmospheric semivolatile organochlorine compounds in European high-mountain areas (Central Pyrenees and High Tatras). *Environ. Sci. Technol.* 38, 3525–3532. doi: 10.1021/es030108p

van Drooge, B. L., and Grimalt, J. O. (2015). Particle size-resolved source apportionment of primary and secondary organic tracer compounds at urban and rural locations in Spain. *Atmos. Chem. Phys.* 15, 7735–7752. doi: 10.5194/acp-15-7735-2015

van Drooge, B. L., Fontal, M., Fernández, P., Fernández, M. A., Muñoz-Arnanz, J., Jiménez, B., et al. (2018a). Organic molecular tracers in atmospheric PM1 at urban intensive traffic and background sites in two high-insolation European cities. *Atmos. Environ.* 188, 71–81. doi: 10.1016/j.atmosenv.2018.06.024

van Drooge, B. L., Ramos García, D., and Lacorte, S. (2018b). Analysis of organophosphorus flame retardants in submicron atmospheric particulate matter (PM1). *AIMS Environ. Sci.* 5, 294–304. doi: 10.3934/environsci.2018.4.294

Venter, Z. S., Aunan, K., Chowdhury, S., and Lelieveld, J. (2020). COVID-19 lockdowns cause global air pollution declines. *Proc. Natl. Acad. Sci. U.S.A.* 117, 18984–18990. doi: 10.1073/pnas.2006853117

Wang, Q., Zhao, H., Wang, Y., Xie, Q., Chen, J., and Quan, X. (2017). Determination and prediction of octanol-air partition coefficients for organophosphate flame retardants. *Ecotoxicol. Environ. Saf.* 145, 283–288. doi: 10.1016/j.ecoenv.2017.07.040

Wegiel, M., Chrzaszcz, R., Maslanka, A., and Grochowalski, A. (2011). Study on the determination of PCDDs/Fs and HCB in exhaust gas. *Chemosphere* 85, 481–486. doi: 10.1016/j.chemosphere.2011.07.079

WHO (2018). *Ambient (outdoor) Air Pollution*. Geneva: WHO.

Wong, F., de Wit, C. A., and Newton, S. R. (2018). Concentrations and variability of organophosphate esters, halogenated flame retardants, and polybrominated diphenyl ethers in indoor and outdoor air in Stockholm, Sweden. *Environ. Pollut.* 240, 514–522. doi: 10.1016/j.envpol.2018.04.086

Zhang, R., Zhang, Y., Lin, H., Feng, X., Fu, T. M., and Wang, Y. (2020). NOx emission reduction and recovery during COVID-19 in East China. *Atmosphere* 11:433. doi: 10.3390/ATMOS11040433

Zhang, W., Ye, Y., Hu, D., Qu, L., and Wang, X. (2010). Characteristics and transport of organochlorine pesticides in urban environment: air, dust, rain, canopy, throughfall, and runoff. *J. Environ. Monit* 12, 2153–2160. doi: 10.1039/C0EM00110D

Zhang, Z., Arshad, A., Zhang, C., Hussain, S., and Li, W. (2020). Unprecedented temporary reduction in global air pollution associated with COVID-19 forced confinement: A continental and city scale analysis. *Remote Sens.* 12:2420. doi: 10.3390/RS12152420

Zhou, L., Hiltscher, M., Gruber, D., and Püttmann, W. (2017). Organophosphate flame retardants (OPFRs) in indoor and outdoor air in the Rhine/Main area, Germany: comparison of concentrations and distribution profiles in different microenvironments. *Environ. Sci. Pollut. Res.* 24, 10992–11005. doi: 10.1007/s11356-016-6902-z

**Conflict of Interest:** The authors declare that the research was conducted in the absence of any commercial or financial relationships that could be construed as a potential conflict of interest.